JOURNAL OF NANO- AND ELECTRONIC PHYSICS
Vol. **6** No 2, 02003(5pp) (2014)

ЖУРНАЛ НАНО- ТА ЕЛЕКТРОННОЇ ФІЗИКИ
Том **6** № 2, 02003(5cc) (2014)

Structural Properties and Elemental Composition of Au^+ Implanted ZnO Films, Obtained by Sol-gel Method

A.D. Pogrebnjak[1,*], T.O. Berestok[1,2,†], A.S. Opanasyuk[1,‡], Y. Takeda[3], K. Oyoshi[3], F.F. Komarov[4], J. Kassi[1]

[1] *Sumy State University, Rimsky-Korsakov St. 2, 40007 Sumy, Ukraine*
[2] *Catalonia Institute for Energy Research, Jardins de les Dones de Negre St. 1, Sant Adria del Besos, 08930 Barcelona, Spain*
[3] *National Institute for Materials Science, Ibaraki St. 305-0047 Tsukuba, Japan*
[4] *Belarusian State University, Independence Ave 4, 220030 Minsk, Belarus*

(Received 30 January 2014; revised manuscript received 06 May 2014; published online 20 June 2014)

The undoped and doped aluminum ZnO films were obtained by sol-gel method onto glass substrates with further implantation of Au^+ ions. RBS, XRD methods and Raman spectroscopy were used for films characterization. The XRD analysis showed that obtained samples have a hexagonal structure with lattice constants $a = 0.3245\text{-}0.3249$ nm, $c = 0.5203\text{-}0.5204$ nm, $c / a = 1.602\text{-}1.603$ and growth texture [101]. The values of coherent scattering domains (CSD) were equal to $L_{(201)} = (13.0\text{-}13.9)$ nm, $L_{(101)} = (12.0\text{-}12.2)$ nm, $L_{(002)} = (11.3\text{-}12.6)$ nm. It is found that there is not observed the effects of Au^+ implantation on the values of CSD, lattice constants and texture of the films. According to X-ray analysis ions of gold in the films are mainly incorporated in the form of phase of $AuZn_3$.

Keywords: ZnO : Al, Implantation Au^+, Sol-gel method, RBS, Raman investigation.

PACS numbers: 81.05.Dz, 81.20.Fw

1. INTRODUCTION

Nowadays, in consequence of unique properties and the possibility of using as a base material of micro-, opto- and acoustoelectronics devices, zinc oxide films attracted the increasing attention of researchers. Zinc oxide has a high transparency in the visible region of the spectrum, a large exciton binding energy, high chemical and thermal stability in the atmosphere [1]. Moreover, due to the large band gap this material can be successfully used as material for LEDs, UV sensors, windows and conductive layers of solar cells, etc. [2-4].

Among the methods of ZnO films obtaining (such as spray pyrolysis [5], vapor deposition [6], chemical bath deposition [7,8]), sol-gel method [9-10] is one of the most promising in order to its simplicity, efficiency and the possibility of layers condensation with different dispersion structure.

To control the luminescent, electrical and optical properties, zinc oxide layers were doped by impurities using different methods. It is expected that improvement of luminescence can be achieved by replacing Zn atoms by heavy-metal atoms like Ag, Cu or Au, which leads to obtaining new luminescence centers in ZnO. It can be explained by heavy-metal ions strong *d* states and the replacing results in increase of the 4*d*-Zn 4*s* optical transitions of ZnO. Synthesis of ZnO doped by Al, Ga, In, Pt, Au has been studied in Refs [11-15].

Among the different methods of films doping, ion implantation is one of the promising methods due to the possibility of creating the defects states and introducing luminescence centers [16-18]. Furthermore, with the help of ion implantation it can reach a high metal filling factor in an irradiated material beyond the equilibrium limit of metal solubility. This method also allows to obtain doping level at various depths under the substrate surface by adjusting implanation energy. Therefore, ZnO implanted with heavy-metal ions can be used for further applications.

Nevertheless, there are many works devoted to synthesis and studying of undoped ZnO films [1-4]. In comparison to this, investigations of the doped layers are uncompleted ones.

Therefore, the purpose of this work is to study the influence of the effect of doping of gold on ZnO films structural and microstructural characteristics. Doping was made using low-energy ion implantation. ZnO films were fabricated by sol-gel method.

2. EXPERIMENTAL DETAILS

Undoped and Al-doped ZnO films were obtained by sol-gel technology [9]. As the basic precursor we used zinc acetate ($Zn(CH_3COO)_2{\cdot}2H_2O$). The solution was prepared by dissolving of zinc acetate in anhydrous methanol, in which polivinilpirrolidon (PVP) was added. Then, resulting solution was mixed for 24 hours at room temperature and filtered. Films were deposited onto glass substrates, which were cleaned in acetone using ultrasound. After rinsing with distilled water, the samples were dried at the temperature of 348 K for 20 min. According to [9], aluminum content was 1-3 % in the doped films.

Doping of ZnO films was carried out by implantation of Au^+ ions with a dose of $10^{16}\text{-}10^{17}$ ion/cm^2 and the beam energy was 60 keV.

* alexp@i.ua
† taisia.berestok@ukr.net
‡ opanasyuk_sumdu@ukr.net

The chemical composition of samples was determined by Raman spectroscopy using Ramanor U1000 spectrometer with a microscope at room temperature. As a source of radiation we used laser LCS-DTL-317 with a wavelength of $\lambda = 532$ nm. Lens with 50 zooms was used for spectra registration.

To obtain information about the elemental composition of the condensates there was used the method of Rutherford backscattering of $^4He^+$ ion. Ion beam energy was 1.4 MeV. Scattering angle was equal to $\theta = 175^o$ at normal incidence of ions at the sample. Energy resolution of the detector was 16 keV. For processing of the spectra and obtaining the depth distribution of elements we used the program SIMNRA.

Structural properties of obtained condensates were investigated using automated diffractometer (Rigaku in Cr-k_a) by sliding beams in the range of diffraction angles 2θ from 20° to 80°, where 2θ is the Bragg angle. In studies, there was used focusing of X-rays according to Bragg-Brentano method. Phase analysis was performed by comparing of interplanar distances and relative intensities of the samples and the standard according to JCPDS [19, 20].

The texture of the films was estimated by the method of Harris, which is especially convenient for tested planar samples with the texture axis that is oriented normally to the surface. Pole density calculated by the formula [21]:

$$P_i = \frac{\left(I_i / I_{0i}\right)}{\frac{1}{N}\sum_{i=1}^{N}\left(I_i / I_{0i}\right)}, \qquad (1)$$

where I_i, I_{0i} is the integrated intensities of the i-th diffraction peak for the film sample and standard; N-number of lines on the diffractogram.

Then on the base of estimation we construct the dependencies $P_i - (hkl)_i$ and $P_i - \varphi$, (where φ is an angle between chosen direction and the normal to different crystallographic planes corresponding to the reflexes in the XRD patterns; (hkl)- Miller indices). Texture axis has the indexes, which corresponds to the highest value of P_i. In this case, the orientation factor for the relevant direction can be calculated from the expression [21]:

$$f = \sqrt{\frac{1}{N}\sum_{i=1}^{N}\left(P_i - 1\right)^2}. \qquad (2)$$

Determination of interplanar distances of wurtzite phase of ZnO was carried out by position of K_{a1} component of all the most intense lines present in the diffractograms.

Calculations of the constants a and c of the hexagonal phase of the material was performed with using appropriate equation [21]:

$$a = \frac{\lambda}{2\sin\theta}\sqrt{\frac{4}{3}(h^2 + hk + k^2) + (a/c)^2 l^2}, \qquad (3)$$

$$c = \frac{\lambda}{2\sin\theta}\sqrt{\frac{4}{3}(a/c)^2(h^2 + hk + k^2) + l^2}, \qquad (4)$$

where λ is the X-ray wavelength and the c/a ratio was considered as constant and it was equal to the value of the ideal lattice constants of hexagonal phase $c / a = 1.633$ [19].

Further values of the lattice constants were clarified using extrapolation method of Nelson- Riley [21]. For this we used the graphical method of successive approximations. Values of lattice constants a and c were determined and the c/a ratio was calculated from the dependences $a(c) - 1/2\cos^2\theta(1/\sin(\theta) + 1/\theta)$. The corresponding values of c / a (c / a) were used to calculate new constants from equations (3) and (4). After this procedure was repeated several times (three to five) until the values a, c and c / a converged [22]. Linear approximation of obtained points was carried out using the method of least squares.

In order to determine the average CSD L in obtained films, Scherrer equations were used [21]:

$$L = \frac{0.94\lambda}{\beta\cos\theta}, \qquad (5)$$

where β is the physical broadening of the diffraction lines.

3. RESULTS AND DISCUSSION

To determine the effectiveness of doping by implantation of gold, there was made an analysis of the elemental composition of the obtained condensates by the RBS method. Fig. 1a shows the energy spectrum of helium ions measured on the sample doped with gold and an example of spectrum modeling. In addition to lines that correspond to the ZnO film and the doping impurity, there are observed lines that correspond to the materials of the glass substrate – Si and O. The presence of lines of gold indicates a result of ion implantation. The depth distribution of the elements in the film is given in Fig. 1b.

As it is shown in Fig. 1 the distribution of aluminium and gold dopants is sufficiently uniform in thickness of the sample. In addition to doping element and elements which form the compound, silicon is present in the sample. It is possible due to diffusion from the substrate.

Using X-ray analysis, we can see, that a line at the angles of 54.97°-55.05° has dominated intensity on the diffractograms of the samples. It corresponds to the reflection from the plane (101) of wurtzite phase of ZnO (Fig. 2) [19]. Moreover, on X-ray patterns there are present sufficiently intensive lines at the angles of 47.95°-48.10° and 52.20°-52.30°, which were identified as reflections from crystallographic planes (100) and (002) of the same phase, respectively. Other lines have lower intensity and correspond to the reflection of crystallographic planes (102), (110), (103), (200), (112), (201), (004), (201), (104) of ZnO with wurtzite structure.

Thus, it was found that the forming of ZnO films onto glass substrate takes place with hexagonal structure. As it is shown in Fig. 2, al peaks are absent in the X-ray patterns of ZnO doped by aluminum. This is due to a small concentration of aluminum and the low sensitivity of XRD method.

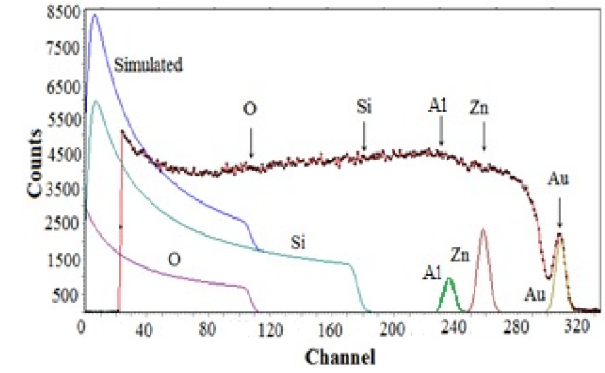

a

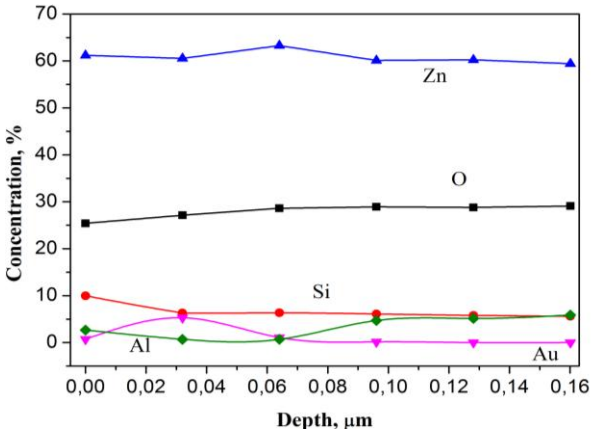

b

Fig. 1 – Energy spectrum of the helium ions scattered on ZnO+Au$^+$ ($E = 6 \times 10^{16}$ ion/cm^2) and examples of simulation (a); the concentration profiles of the elements in the film (b)

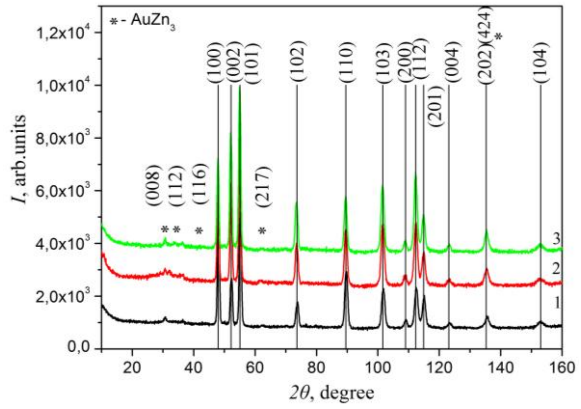

Fig. 2 – XRD patterns of the ZnO (2, 3) and ZnO:Al (1) doped by Au$^+$ imlantation

The reverse pole figures calculation allowed revealing the existence of the texture growth [101] in obtained condensates. Texture had low quality and the orientation factor did not exceed the values of $f = 0.75$-0.80. Type of the texture and the quality did not change after gold implantation

Moreover, in the X-ray patterns of the Au doped samples the peaks were fixed at 31.69°, 34.69°, 41.65°, 62.31°, and 135.48° angles with low intensity. They have been identified as a reflection of the plane (008), (112), (116), (217) and (424) of cubic phase of the compound $AuZn_3$. These lines are the most intensive on X-ray pattern at reflections of Ref [20] (PDF № 12-0084). Atomic weight of gold is higher than aluminum atomic weight, therefore line of compounds containing gold is observed in diffraction pattern, although at the limit of sensitivity of the method. In Ref [13] authors investigated nanostructured ZnO films deposited on gold sublayer, the additional lines after annealing of structures were also observed. Thus, according to the results of X-ray analysis, gold atoms are incorporated into a chemical bonding with zinc with the further formation of $AuZn_3$.

The results of lattice constant calculations for doped and undoped ZnO condensates are presented in Table 1. The value of the lattice constants a, c and the ratio c / a are practically unchanged after the first iteration. This indicates on finding of the procedure of constants calculation. It is established that the values of the lattice constant of the material ($a = 0.3245$-0.3249 nm, $c = 0.5203$-0.5205 nm, $c / a = 1.602$-1.603) are in the reasonable agreement with the data given in Ref [15] ($a = 0.3249$ nm; $c = 0.5205$ nm, $c / a = 1.602$) [15]. As it is seen in Table 1, we can not find changes of the lattice constants of the material after the implantation of gold. These results correlate with the data of X-ray analysis, which indicate on the formation of a new phase containing gold – $AuZn_3$.

Results of determination of grain size of ZnO film by reflections from crystallographic planes (100), (002), (101) and (201) are shown in Table 1. It is found, that average size of CSD has approximately the same value in all directions, which indicates on the sphericity of these entities. Thus, implantation of Au did not led to significant changes in the lattice constants and in the CSD size of the material.

Table 1 – Calculation results of lattice constants and CSD of ZnO films

Sample	Lattice constant, a, c, nm			Grain size L, nm			
				hkl			
	a	c	c / a	(100)	(002)	(101)	(201)
ZnO : Al, Au	0.3245	0.5204	1.603	13.4	11.3	12.0	13.9
ZnO : Au	0.3246	0.5204	1.603	13.6	12.6	12.2	13.0
ZnO : Au	0.3248	0.5203	1.602	13.3	12.4	12.2	13.8
Ref. [19, 20]	0.3249	0.5205	1.602				

This is due to lack of recrystallization processes and allocation of gold in a separate phase.

One of the most effective methods of determining the material crystallinity is Raman spectroscopy. It is well known, ZnO with C^4_{6v} space group has two formula units per primitive cell. Eight sets of optical phonon modes were classified at the Γ point of the Brillouin zone: $A_1 + E_1 + 2E_2$ modes (Raman active) where modes A_1 and E_1 are polar and $2E_2$ (E_2^{low} and E_2^{high}) – nonpolar, $2B_1$ modes (Raman silent) and $A_1 + E_1$ modes (infrared active). The E_1 mode is splitted into transverse optical (TO), and longitudinal optical (LO) branches.

A typical Raman scattering spectrum of the sample is shown in Fig. 3.

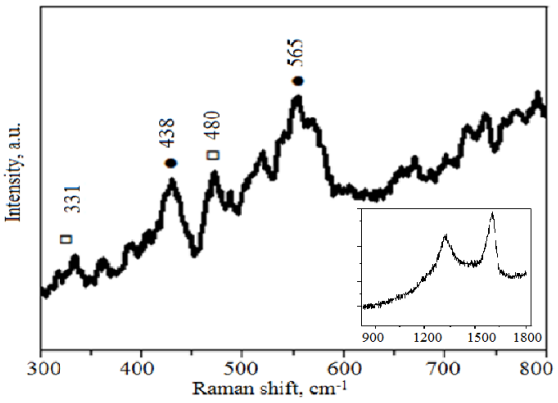

Fig. 3 – Raman spectra of (ZnO / glass + Au) sample

There are several peaks at frequencies of 331, 433, 480, 565, 1326 and 1588 cm^{-1} in the spectra. According to Ref [12] in the experimental spectra peaks are interpreted as belonging to the hexagonal phase of ZnO: $2E_2$(M) – 331 cm^{-1}; E_2^{high} – 433 cm^{-1} that corresponding to the non-polar modes; A_1(LO) – 565 cm^{-1} – corresponds to the polar mode. Peaks, located at frequencies of 1326 cm^{-1} and 1588 cm^{-1}, correspond to peaks of D and G – carbon groups, respectively. Unfortunately, the peaks belonging to $AuZn_3$ phase were not detected.

4. CONCLUSIONS

ZnO : Al films were obtained by sol-gel method and further doped by Au^+ using ion implantation. Obtained samples were investigated by RBS methods, X-ray diffraction analysis and Raman spectroscopy. According to the RBS the distribution of aluminum and gold dopant is sufficiently uniform over the thickness of the samples. With the help of XRD-method it was shown that films have a hexagonal structure with textured growth of [101]. It was found that the average size of CSD has almost the same values in all crystallographic directions, which correspond to the axes of the hexagonal lattice phase ($L_{(201)}$ = (13.0-13.8) nm, $L_{(101)}$ = (12.0-12.2) nm, $L_{(202)}$ = (11.3-12.6) nm). Moreover, we calculated the precise values of lattice constants by Nelson-Raleigh method (a = 0.3245-0.3248 nm, c = 0.5203-0.5204 nm, c / a = 1.602-1.6603) and obtained the values corresponding to the data listed in the literature.

We did not observe effects of Au^+ implantation on the value of CSD sizes, lattice constants and texture of the films. This suggests that the process of implantation of gold is not accompanied by recrystallization processes in the samples. According to X-ray analysis ions of gold in the films are present mainly in the form of phase of $AuZn_3$.

AKNOWLEDGEMENTS

This research was supported by the Ministry of Education and Science of Ukraine (Grant No. 0110U001151) and the Ukraine State Agency of the Science, Innovation and Informatization as well as by the NRF grant funded by the MEST of Korea within the project «Advanced materials for low-cost high-efficiency polycrystalline heterojunction thin films solar cells».

Структурні властивості та елементний склад імплантованих Au^+ плівок ZnO:Al, отриманих золь-гель методом

О.Д. Погребняк[1], Т.О. Берестok[1,2], А.С. Опанасюк[1], Y. Takeda[3], K. Oyoshi[3], F.F. Komarov[4], J. Kassi[1]

[1] *Сумський державний університет, вул. Римського-Корсакова, 2, 40007 Суми, Україна*
[2] *Catalonia Institute for Energy Research, Jardins de les Dones de Negre St. 1, Sant Adria del Besos, 08930 Barcelona, Spain*
[3] *National Institute for Materials Science, Ibaraki St. 305-0047 Tsukuba, Japan*
[4] *Білоруський державний університет, пр. Незалежності, 4, 220030 Мінськ, Беларусь*

Методами RBS, рентгеноструктурного аналізу та раманівського розсіювання були досліджені леговані та нелеговані алюмінієм плівки ZnO, отримані за допомогою золь-гель методу на скляних підкладках з подальшим імплантуванням іонами Au^+. Рентгенодифрактометричний аналіз показав, що зразки мають гексагональну структуру з постійними гратки a = 0.3245-0.3248 нм, c = 0.5203-0.5204 нм, c / a = 1.602-1.603 та текстурою росту [101]. Середній розмір ОКР в зразках становить $L_{(100)}$ = 13.3-13.6 нм, $L_{(002)}$ = (11.3-12.6) нм, $L_{(101)}$ = 12.0-12.2 нм. Встановлено, що розмір ОКР, період гратки та якість текстури отриманих зразків не залежать від імплантування плівок ZnO іонами Au^+. За даними рентгеноструктурного аналізу показано, що іони золота у плівках знаходяться в основному у вигляді фази $AuZn_3$.

Ключові слова: ZnO:Al, імплантування Au^+, золь-гель метод, RBS, Раманівська спектроскопія.

Структурные свойства и элементный состав имплантированных Au^+ пленок ZnO:Al, полученных золь-гель методом

А.Д. Погребняк[1], Т.А. Берестok[1,2], А.С. Опанасюк[1], Y. Takeda[3], K. Oyoshi[3], Ф.Ф. Комаров[4], J. Kassi[1]

[1] *Сумский государственный университет, ул. Римского-Корсакова, 2, 40007 Сумы, Украина*
[2] *Catalonia Institute for Energy Research, Jardins de les Dones de Negre St. 1, Sant Adria del Besos, 08930 Barcelona, Spain*
[3] *National Institute for Materials Science, Ibaraki St. 305-0047 Tsukuba, Japan*
[4] *Белорусский государственный университет, пр. Независимости, 4, 220030 Минск, Беларусь*

Методами RBS , рентгеноструктурного анализа и рамановского рассеяния были исследованы легированные и нелегированные алюминием пленки ZnO, полученные с помощью золь - гель метода на стеклянных подложках с последующим имплантированием ионами Au^+. Рентгенодифрактометрический анализ показал, что образцы имеют гексагональную структуру с постоянными решетки a = 0.3245-0.3248 нм, c = 0.5203-0.5204 нм, c / a = 1.602-1.603 и текстурой роста [101]. Средний размер ОКР в образцах составляет $L_{(100)}$ = 13.3-13.6 нм , $L_{(002)}$ = (11.3-12.6) нм , $L_{(101)}$ = 12.0-12.2 нм. Установлено, что размер ОКР, период решетки и качество текстуры полученных образцов не зависят от имплантирования пленок ZnO ионами Au^+. По данным рентгеноструктурного анализа показано, что ионы золота в пленках находятся в основном в виде фазы $AuZn_3$.

Ключевые слова: ZnO:Al, имплантация Au^+, золь-гель метод, RBS, Рамановская спектроскопия.

REFERENCES

1. F.A. Wei, L. Pan, W. Huang, *Mater. Sci. Eng. B* **176**, 1409 (2011).
2. U. Özgür, Ya.I. Alivov, C. Liu, A. Teke, M.A. Reshchikov, S. Doğan, V. Avrutin, S.-J. Cho, H. Morkoç, *J. Appl. Phys.* **98**, 041301 (2005).
3. C. Klingshirn, *phys. status solidi b* **244**, 3027 (2007).
4. I.I. Shtepelyuk, G.V. Lashkaryov, V.Y. Lazorenko, *Phys. Chem. Solids* **11(2)**, 277 (2010).
5. A. Bougrine, A.E. Hichou, M. Addou, J. Ebothé, A. Kachouane, M. Troyon, *Mater. Chem. Phys.* **80**, 438 (2003).
6. A.D. Pogrebnjak, N.Y. Jamil, A.K.M. Muhammed, *VisnykKhNU* **962**, 58 (2011).
7. T.M. Barnes, J. Leaf, C. Fry, C.A. Wolden, *J. Crystal Growth* **274**, 412 (2005).
8. T.O. Berestok, D.I. Kurbatov, N.M. Opanasyuk, A.D. Pogrebnjak, O.P. Manzhos, S.M. Danilchenko, *J. Nano- Electron. Phys.* **5 (1)**, 01009 (2013).
9. A.D. Pogrebnjak, A.A. Muhammed, E.T. Karash, N.Y. Jamil, J. Partyka, *Prz. Elektrotechniczn.* **3b**, 315 (2013).
10. V. Kumari, B.P. Malik, D. Mohan, R.M. Mehra, *J. Nano-Electron. Phys.* **3**, 601 (2011).
11. A.C. Aragones, A. Palacios-Padros, F. Caballero-Briones, F. Sanz, *Electrochim. Acta* **109**, 117 (2013).
12. S. Kahraman, H.M. Cakmak, S. Cetinkaya, F. Bayansal,H.A. Cetinkara, H.S. Guder, *J. Crystal Growth* **363**, 86 (2012).
13. F. Jamali-Sheini, R. Yousefi, K.R. Patil, *Ceram. In.* **38**, 6665 (2012).
14. X.D. Zhang, P. Wu, Y.Y. Shen, L.H. Zhang, Y.H. Xue, F. Zhu, D.C. Zhang, C.L. Liu, *Appl. Surf. Sci.* **258**, 151 (2011).
15. L. Wang, J. Wang, S. Zhang, Y. Sun, X. Zhu, Y. Cao, X. Wang, H. Zhang, *Anal. Chim. Acta* **653**, 109 (2009).
16. F. Reuss, C. Kirchner, Th. Gruber, R. Kling, S. Marschek, W. Limmer, A. Waag, P. Ziemann, *J. Appl. Phys.* **95**, 3385 (2004).
17. T.S. Jeong, M.S. Han, C.J. Youn, Y.S. Park, *J. Appl. Phys.* **96**, 175 (2004).
18. K. Lorenz, E. Alves, E. Wendler, O. Bilani, W. Wasch, H. Hayes, *Appl. Phys. Lett.* **87**, 191904 (2005).
19. Selected powder diffraction data for education straining (Search manual and data cards)], Published by the International Centre for diffraction data, USA.**63**, 442, (1993).
20. Selected powder diffraction data for education straining (Search manual and data cards)], Published by the International Centre for diffraction data, USA.**49**, 234 (1958).
21. Ja.S. Umanskij, Ju.A. Skakov, A.N. Ivanov, L.N. Rastorgujev, *Crystallogaphy, X-ray graph and electronmicroscopy* (Metallurgy: Moskow: 1982), [in Russian].
22. V.V. Kosyak, D.I. Kurbatov, M.M. Kolesnyk, et al., *Mater. Chemis. Phys.* **138**, 731 (2013).